OPEN ACCESS
CellPress

Cell Reports
Article

Polarized Expression of p75^{NTR} Specifies Axons during Development and Adult Neurogenesis

Emanuela Zuccaro,[1,6,7] Matteo Bergami,[1,2,7] Beatrice Vignoli,[1,7] Guillaume Bony,[1] Brian A. Pierchala,[3] Spartaco Santi,[4] Laura Cancedda,[1,*] and Marco Canossa[1,5,*]

[1]Department of Neuroscience and Brain Technologies, Italian Institute of Technology (IIT), via Morego 30, I-16163 Genoa, Italy
[2]Cologne Excellence Cluster on Cellular Stress Responses in Aging-Associated Diseases (CECAD), University Hospital of Cologne, Joseph-Stelzmann-Strasse 26, Cologne, Germany
[3]Department of Biologic and Materials Sciences, University of Michigan School of Dentistry, 1011 N. University Avenue, Ann Arbor, MI 48109, USA
[4]National Research Council (CNR), Institute of Molecular Genetics (IGM)-Bologna, Laboratory of Muscoloskeletal Cell Biology, IOR, via di Barbiano1/10, I-40136 Bologna, Italy
[5]European Brain Research Institute (EBRI) "Rita Levi-Montalcini," via del Fosso di Fiorano 64/65, I-00143 Rome, Italy
[6]Present address: Department of Stem Cell and Regenerative Biology, Harvard University, Cambridge, MA 02138, USA
[7]Co-first authors
*Correspondence: marco.canossa@iit.it (M.C.), laura.cancedda@iit.it (L.C.)
http://dx.doi.org/10.1016/j.celrep.2014.02.039

SUMMARY

Newly generated neurons initiate polarizing signals that specify a single axon and multiple dendrites, a process critical for patterning neuronal circuits in vivo. Here, we report that the pan-neurotrophin receptor p75^{NTR} is a polarity regulator that localizes asymmetrically in differentiating neurons in response to neurotrophins and is required for specification of the future axon. In cultured hippocampal neurons, local exposure to neurotrophins causes early accumulation of p75^{NTR} into one undifferentiated neurite to specify axon fate. Moreover, knockout or knockdown of p75^{NTR} results in failure to initiate an axon in newborn neurons upon cell-cycle exit in vitro and in the developing cortex, as well as during adult hippocampal neurogenesis in vivo. Hence, p75^{NTR} governs neuronal polarity, determining pattern and assembly of neuronal circuits in adult hippocampus and cortical development.

INTRODUCTION

Neuronal polarization is critical for neural network formation during brain development, yet the mechanisms used by neurons to specify and direct axon growth are poorly understood. Growth cones located at the tips of undifferentiated neurites detect and respond to environmental cues. This leads to activation of intracellular signaling cascades and causes a single neurite to grow longer than the others, ultimately becoming the axon (Craig and Banker, 1994; Arimura and Kaibuchi, 2007; Barnes et al., 2008; Tahirovic and Bradke, 2009; Cáceres et al., 2012; Cheng and Poo, 2012). Of the chemical cues known to govern neurite outgrowth, the neurotrophins nerve growth factor (NGF), brain-derived neurotrophic factor (BDNF), neurotrophin-3 (NT-3), and neurotrophin-4/5 (NT-4/5) are particularly promising candidates for axonal specification (Cheng and Poo, 2012).

p75^{NTR} binds to and is activated by all members of the neurotrophin family (Bibel and Barde, 2000; Huang and Reichardt, 2001). Although p75^{NTR} is a known trigger of programmed cell death (Roux and Barker, 2002), it can also act as a receptor for controlling axon growth (Dechant and Barde, 2002; Schecterson and Bothwell, 2008, 2010). In particular, the effects of neurotrophins and p75^{NTR} on neurite growth involve interaction with the protein kinase Rho. When neurotrophins bind to p75^{NTR}, Rho activity is diminished, and this favors axonal growth. p75^{NTR} can also regulate neurite growth via other mechanisms. p75^{NTR} can suppress the repellant action of Semaphorin 3A (Sema3A) on axon growth in a neurotrophin-independent fashion (Ben-Zvi et al., 2007). p75^{NTR} suppress Sema3A actions by inhibiting plexin-neuropilin elongation in myelin-rich areas where axons normally would not grow (Walsh et al., 1999), and it also mediates myelin-induced collapse of axon growth cones (Wang et al., 2002; Wong et al., 2002; Kaplan and Miller, 2003; Yamashita and Tohyama, 2003; Park et al., 2010). Notably, the Sema3A pathway has been recently involved in axonal polarization (Shelly et al., 2011). Moreover, in response to binding of specific ligands to Nogo receptor, p75^{NTR} (Wang et al., 2002; Wong et al., 2002) and Lingo-1 (Mi et al., 2004) are recruited to form a ternary complex that prevents the cytoskeletal changes necessary for axonal elongation and specification (Neukirchen and Bradke, 2011; Wu et al., 2012). Finally, p75^{NTR} promotes axon degeneration after the axon terminal arrives to the target tissue during developmental pruning (Singh et al., 2008). These findings highlight an important role for p75^{NTR} in controlling axonal outgrowth and suggest a possible role for p75^{NTR} in neuronal polarization.

Here, we present clear in vitro and in vivo experimental evidence demonstrating that p75^{NTR} plays a pivotal role in axonal specification.

RESULTS

Polarized Distribution of p75^{NTR} Preludes Axonal Specification

To specify a single axon from one of several undifferentiated neurites, polarizing proteins are selectively localized into the process that will eventually become the axon (Arimura and Kaibuchi, 2007). We predicted that pan-neurotrophin p75^{NTR} would be preferentially expressed in the neurite that assumes axonal identity. To test this hypothesis, we prepared cultures of dissociated hippocampal neurons from embryonic day 17 (E17) mice. Undifferentiated neurons, visualized by transfection of GFP, extended several nascent neurites with similar lengths during the first 24 hr after plating. In transfected neurons, we normalized p75^{NTR} immunoreactivity to GFP signal to account for cytoplasmic volume variation and ensure reliable quantification of preferential p75^{NTR} localization in single processes. At 6 hr after plating, we observed high p75^{NTR} immunofluorescence in one—and only one—neurite in 28% ± 3% of the neurons (Figures 1A and 1B). Localization of p75^{NTR} in one single neurite was observed in 42% ± 4% of the cells 12 hr after plating (Figure 1B). At the time of polarity breaking (24–48 hr), the proportion of cells expressing p75^{NTR} in a single process increased (59% ± 9%, 24 hr; 72% ± 2%, 48 hr), reaching a plateau (76% ± 9%) at 72 hr, when neurons acquired a polarized morphology in culture (Figure 1B). Moreover, the number of neurons with no p75^{NTR} expression decreased, and the number of cells expressing p75^{NTR} in multiple processes did not significantly change over the 72 hr time period (Figure 1B). The hypothesis that polarized p75^{NTR} accumulation is a prelude to axonal specification was further supported by simultaneously labeling neurons with antibodies for the axon-specific marker Smi312 and for p75^{NTR}. The vast majority (approximately 80%–90%) of the cells expressing p75^{NTR} in a single process showed clear colocalization with the axonal marker (Figure 1C). Accumulation of p75^{NTR} in axons followed a specific pattern as axon differentiation progressed. Indeed, the magnitude of receptor expression increased from 24 to 48 hr reaching the maximum intensity after 72 hr. Notably, after polarization (120 hr), p75^{NTR} was expressed at similarly low levels in all neurites with the exception of the axon tip, where p75^{NTR} labeling was still observed at high levels (Figure 1D). Thus, transient accumulation of p75^{NTR} in a single neurite represents a temporal and spatial landmark that preludes axonal specification.

The identity of an axon is somewhat flexible (Arimura and Kaibuchi, 2007): cutting the axon of an already-polarized neuron can result in the specification of a new axon at the expense of minor neurites (Dotti and Banker, 1987; Gomis-Rüth et al., 2008; Toriyama et al., 2010). Because p75^{NTR} distribution is predictive of axonal specification, we hypothesized that its expression would decrease in a lesioned axon and accumulate in the neurite acquiring a new axonal identity. Consistent with this assumption, 6 hr after injury, p75^{NTR} was absent at the stump of transected axons but present in other neurites in 73% ± 4% of the cells (Figure 1E). Accumulation of p75^{NTR} in the new axon was confirmed 72 hr after axotomy (Figure 1F; see also Movie S1). We next tested whether axonal injury that does not change axonal specification would alter p75^{NTR} expression. Cutting the axon at a long distance from the cell body prevents a new neurite from becoming the axon (Dotti and Banker, 1991; Goslin and Banker, 1989; Takahashi et al., 2007). Indeed, axonal expression of p75^{NTR} was preserved when the axon was cut at a distance greater than five times the cell diameter (Figure 1E). Therefore, p75^{NTR} expression precedes conversion of neurites to axons following axotomy.

Localized Exposure of Neurotrophins Results in Polarized p75^{NTR} Distribution and Subsequent Axonal Specification

Although the accumulation of p75^{NTR} in the fated axon appeared stochastic in our cultured neurons, neurotrophins might provide an external signal orienting axonal specification via p75^{NTR}. We addressed this possibility by culturing neurons on coverslips patterned with NGF, NT-3, or BDNF stripes and determining whether axon initiation was oriented at the stripe border toward the neurotrophins. Live-cell imaging revealed that after a period of dynamic neurite growth spurts and retractions, axons (defined as processes of $\geq$ five times cell diameter in length) preferentially extended toward the neurotrophin stripes (Figure 2A; see also Movie S2). The preferred direction of axon extension was quantified using a preference index (PI; [% on stripe] − [(% off stripe)/100%]) (Shelly et al., 2007). Neurons cultured on coverslips patterned with control BSA stripes displayed similar axon growth on and off the stripes (Figure 2A).

To determine whether neurotrophin influence on axon initiation requires selective binding to p75^{NTR}, we added a α-p75-blocking antibody (Weskamp and Reichardt, 1991; Huber and Chao, 1995) to the culture medium. The antibody abolished the preference of axons for initiation on BDNF stripes, as determined by morphological analysis (Figure 2A) and Smi312 labeling (Figure 2B). The blocking effect of α-p75 antibody also extended to NGF and NT-3 stripes (Figure 2B), indicating that all neurotrophins require p75^{NTR} to orient axon specification.

If accumulation of p75^{NTR} in the fated axon predicts axonal identity, we expect that initial asymmetry in p75^{NTR} distribution is oriented in the fated axon before the polarity breaking point. Indeed, we found that neurites expressing higher levels of p75^{NTR} preferentially extended toward neurotrophin stripes as early as 12 hr after plating (Figure 2C), indicating selective p75^{NTR} localization in the fated axon far before that axon is specified. Later in differentiation, colocalization of p75^{NTR} and Smi312 immunoreactive signals was conserved in the process that preferentially oriented toward the neurotrophin stripes. Taken together, these results provide clear evidence that p75^{NTR} accumulation precedes axonal specification, which in turn is regulated by neurotrophins. Moreover, these data suggest a positive-feedback loop between local p75^{NTR} activation and receptor-localized accumulation (Figure 2D).

Polarized Localization of p75^{NTR} Is Required for Axonal Initiation

To determine if the polarized localization of p75^{NTR} is necessary to initiate an axon, we knocked down p75^{NTR} by RNAi in neuronal hippocampal cultures at plating. The vectors expressing short hairpin RNA (shRNA) against p75^{NTR} (sh-p75) also drove the

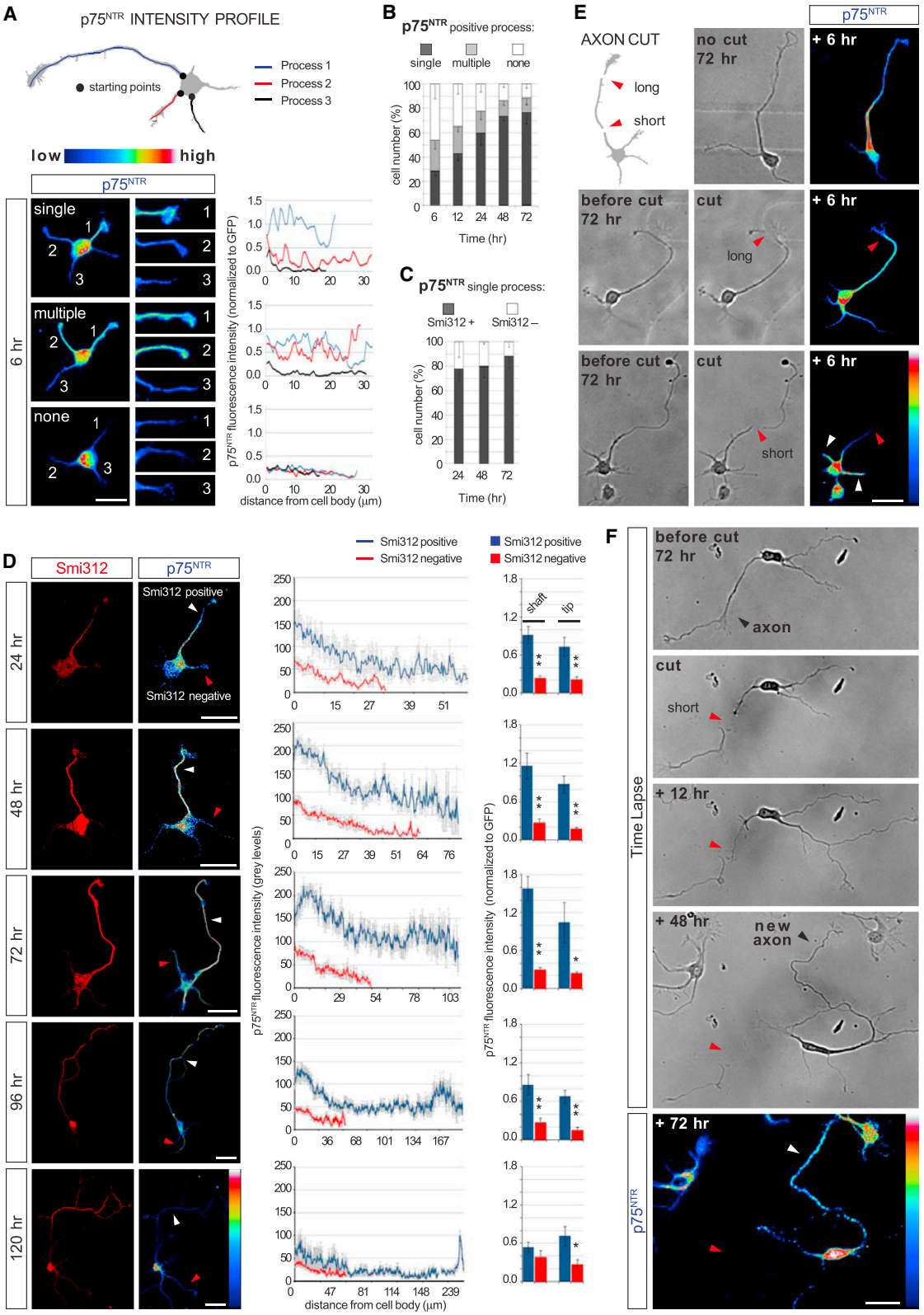

(legend on next page)

expression of red fluorescent protein (RFP) to allow normalization of $p75^{NTR}$ immunoreactivity in transfected cells. We then determined the effects of $p75^{NTR}$ knockdown on axonal differentiation. Because $p75^{NTR}$ immunofluorescence is heterogeneous in control neurons after 72 hr, we assumed that knockdown of $p75^{NTR}$ would be functionally significant for axonal specification only when $p75^{NTR}$ is decreased below statistical variation (cutoff value in Figure 3B). Accordingly, reductions of $p75^{NTR}$ expression below cutoff correlated with the absence of a single long process labeled by the axon-specific marker Smi312 after 72 hr. These neurons contained three or more neurites of similar length and expressed residual low $p75^{NTR}$ signals equally visible in all processes (Figure 3A). The transfected cells that showed downregulation of $p75^{NTR}$ above cutoff (Figure 3B) displayed Smi312 labeling in a single, long process (Figure 3A). Control neurons transfected with scrambled shRNA exhibited the greatest level of $p75^{NTR}$ labeling in axons (Figure 3B). Quantitative analysis (Figure 3C) revealed that after 72 hr in culture, we observed an overall phenotype characterized by (1) an increased percentage of neurons lacking the axon (44% ± 1%) in sh-p75 cells compared to control cells (11% ± 2%), (2) a decreased number of neurons expressing a single axon (43% ± 2%) compared to controls (78% ± 3%), and (3) no significant change in the number of cells expressing multiple axons. Remarkably, the majority (79% ± 3%) of the Smi312-negative neurons expressed $p75^{NTR}$ levels below cutoff after 72 hr. Thus, our data indicate that threshold $p75^{NTR}$ expression at the polarity breaking highly correlates with the axonal phenotype of sh-p75 neurons. The polarity defect of sh-p75 neurons persisted even when cells were exposed to striped BDNF, clearly supporting the notion that neurotrophins require $p75^{NTR}$ signaling to initiate axons in immature neurons (Figure 3G).

Experiments where we knocked out *$p75^{NTR}$* gene in embryonic hippocampal culture from $p75^{lox/lox}$ mice confirmed that $p75^{NTR}$ is a key player in axonal specification. Mice were generated by flanking exons 4–6 of the *$p75^{NTR}$* gene with loxP sites (Bogenmann et al., 2011). Neuronal cultures from $p75^{lox/lox}$ mice were transfected with vectors expressing Cre-recombinase-GFP or the reporter gene GFP as a control (Figures 3D–3F). In contrast to the polarized distribution of endogenous $p75^{NTR}$ in control cells (78% ± 2% single; 12% ± 1% none), Cre-positive neurons (41% ± 1% single; 47% ± 1% none) expressing $p75^{NTR}$ levels below the cutoff failed to form an appreciable Smi312-positive axon after 72 hr.

To specifically disrupt polarized expression of $p75^{NTR}$, we overexpressed GFP-tagged $p75^{NTR}$ (p75-GFP) (Bergami et al., 2008b). In contrast to the polarized distribution of endogenous $p75^{NTR}$, neurons transfected with p75-GFP showed uniform distribution of fluorescence in the cell body and nearly all the processes (Figure 4A). These neurons failed to form an appreciable Smi312-positive axon in both regular (Figure 4A) and neurotrophin stripe cultures (Figure 4B). Similar results were observed for neurons transfected with wild-type (WT) $p75^{NTR}$ after 72 hr (data not shown), indicating that GFP fused to $p75^{NTR}$ receptor does not interfere with the effect of p75-GFP overexpression. These data demonstrate that preferential subcellular localization of $p75^{NTR}$ in a single neurite is necessary for the correct polarization of neurons in cultures.

Next, we performed live imaging to gain insights into the dynamic processes (neurites extension/retraction overtime) by which sh-p75 knockdown (Figure 3H; see also Movie S3) or p75-GFP (Figure 4C; see also Movie S4) transfection of neurons from WT mice and Cre-GFP (Figure 3H) transfection of neurons from $p75^{lox/lox}$ mice affect the morphological changes that accompany neurite outgrowth and specification. Active extension/retraction was quantified by measuring the number of events over 72 hr. The identity of neurites (axon and dendrites) was defined according to their final length. Observation of cells between 24 and 72 hr in culture revealed that control neurons extend (ext) and retract (ret) their neurites (41 ± 3 ext/ret) until they showed a break in their original symmetry, extending one axon that underwent a period of progressive growth. In contrast, sh-p75-transfected (40 ± 2 ext/ret), Cre-GFP-transfected (43 ± 2 ext/ret), or p75-GFP-transfected (49 ± 1 ext/ret) neurons continued to display similar dynamic elongation and retraction of short neurites, without overgrowth of one single long process.

Overall, our data indicate that the key events underlying specification of a morphologically defined axon require polarized expression of $p75^{NTR}$ at the polarity breaking point.

$p75^{NTR}$ Specifies Axons in Neurons Generated from Adult Hippocampal Progenitor Cells upon Cell-Cycle Exit In Vitro

Assessment of neuronal polarization in dissociated hippocampal neurons typically relies on postmitotic neurons that were previously polarized in vivo. It is possible that in culture these neurons reactivate only a portion of the original polarity programs. Ideally, polarization should be investigated in neurons generated from

Figure 1. Polarized Distribution of $p75^{NTR}$ Precedes Axonal Specification

(A) Pseudocolor images of neurons stained for $p75^{NTR}$. Right panels show processes 1 to 3 for each neuron. Profile of $p75^{NTR}$ fluorescence intensity is reported for each process. Scale bar represents 20 μm.

(B) Percentage of cells showing preferred $p75^{NTR}$ localization in a single neurite, multiple neurites, or no neurite. Data depict average percentage (±SEM) from 17 different cultures (~60–80 cells each) for different time points.

(C) Average percentage showing $p75^{NTR}$ and Smi312 colocalization in one single process (from B) at different times.

(D) Representative confocal or pseudocolor images of neurons stained for Smi312 and $p75^{NTR}$, respectively. $p75^{NTR}$ intensity profiles are reported on the right of each analyzed neuron. Histograms show $p75^{NTR}$ fluorescence intensity normalized to that of GFP at the shaft and tip of Smi312-positive and Smi312-negative processes. Data depict average percentage (±SEM) from nine different cultures (~25 cells each) (*$p < 0.05$; **$p < 0.01$). Scale bar represents 20 μm.

(E) Transmitted light image of neurons before and after the axon has been cut. Pseudocolor images show the same neurons stained for $p75^{NTR}$ 6 hr after cuts. White arrows indicate $p75^{NTR}$ expression in dendrites. Scale bar represents 20 μm.

(F) Sequential images showing a neuron before and after an axon has been cut (red arrow). After 48 hr, one of the short neurites at the time of the axon transection had grown into a new axon, which showed high $p75^{NTR}$ fluorescence after 72 hr. Scale bar represents 20 μm.

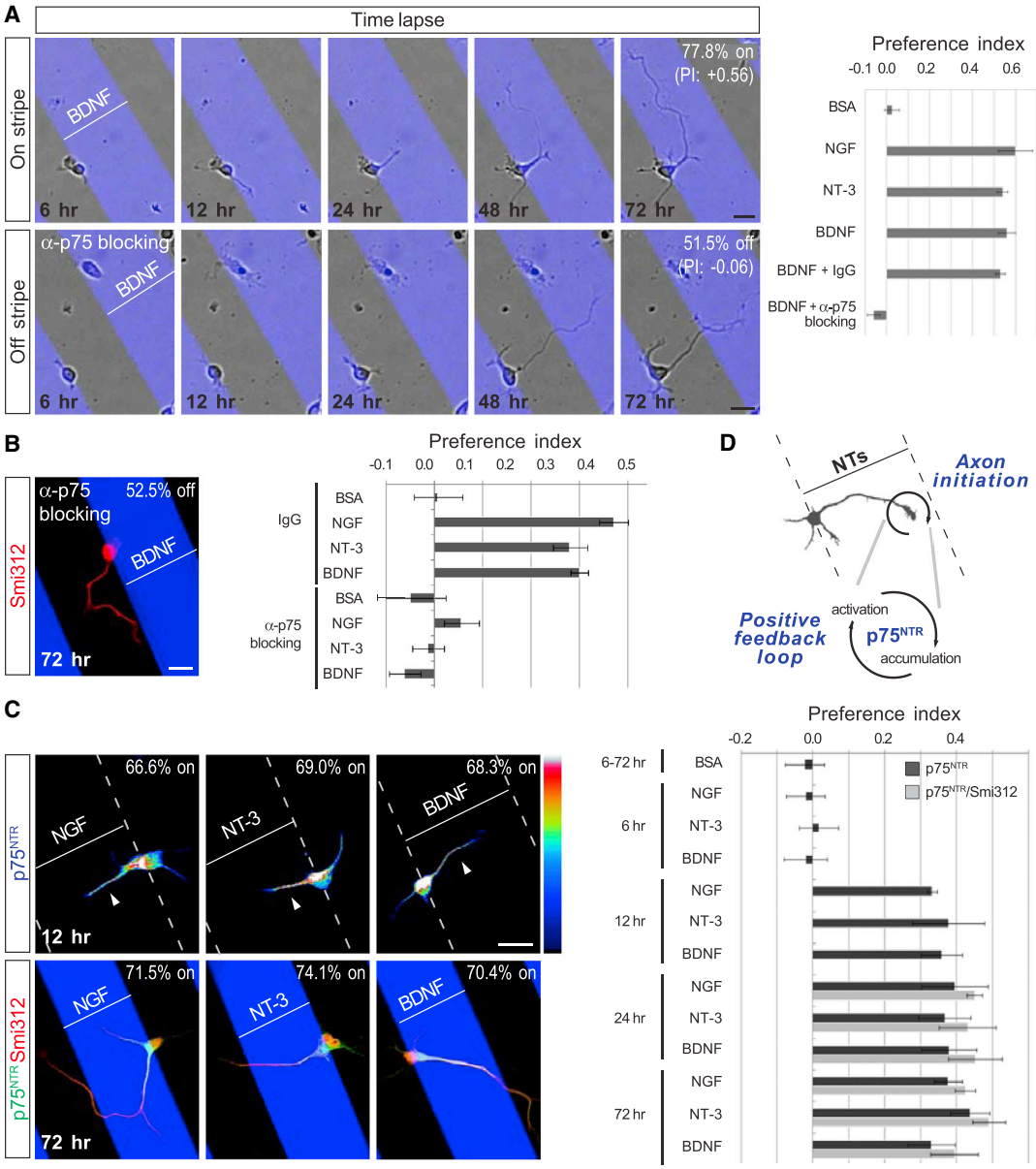

Figure 2. Neurotrophins Localize and Accumulate p75^{NTR} in One Neurite to Specify Axon Fate

(A) Sequential images showing neurons cultured on alternate patterns of poly-L-lysine (gray) and BDNF (blue) stripes in the absence or presence of α-p75 blocking antibody. Neurons at the stripe boundary grow the axon on or off a BDNF stripe. Histograms represent the preference index quantification. Data depict average percentage (±SEM) from three different cultures (~30–40 cells each) for each condition. Scale bar represents 10 μm.

(B) Representative neuron that had grown the axon off BDNF stripes in the presence of α-p75-blocking antibody. Histograms represent preference index quantification. Data depict average percentage (±SEM) from 11 different cultures (~30–40 cells each) for each condition. Scale bar represents 20 μm.

(C) Pseudocolor or confocal images of neurons stained for p75^{NTR}. Dashed lines limit neurotrophin stripes. Arrowheads indicate p75^{NTR} fluorescence accumulated in neurites. Histograms represent the preference index quantification of axon growth. Data depict average percentage (±SEM) from ten different cultures (~50–60 cells each) for each time point. Scale bar represents 20 μm.

(D) The schematic diagram depicts one neuron at a stripe boundary (dashed lines). Continuous NT-induced activation followed by accumulation of p75^{NTR} creates a positive-feedback loop.

progenitor cells after their last mitotic division in vitro. To address this issue, we purified progenitor cells from the dentate gyrus of adult mice. Cells were maintained in a proliferative state by adding fibroblast growth factor (FGF) and epidermal growth factor (EGF), and then they were induced to differentiate by sequential growth-factor withdrawal (Babu et al., 2007). Figure 5A shows a typical progenitor cell with a glial-like shape that generated two immature neurons. The newborn cell showed polarized

morphology immediately after cell division, with a single long process at one pole and one or more shorter processes at the opposite pole. At this stage, polarity was a dynamic process (Figure 5A; see also Movie S5), as the newborn cell exchanged its polar orientation over time until it acquired the stable morphology of a doublecortin (Dcx-positive) neuron expressing one Smi312-positive axon after 7 days in vitro (div).

After characterization of polarity transitions in progenitor cell cultures, we assessed whether $p75^{NTR}$ is required to determine axon fate in newborn neurons generated in vitro. Cells were transfected with scrambled shRNA or sh-p75 in progenitors from WT mice and GFP or Cre-GFP from $p75^{lox/lox}$ mice and plated to allow axonal differentiation (Figure 5B). In contrast to the generation of a single Smi312-positive axon in most control cells (scrambled shRNA: 61% ± 3% single versus 18% ± 4% none; GFP: 59% ± 4% single versus 21% ± 3% none), a higher portion of sh-p75- and Cre-GFP-transfected neurons grew undifferentiated, Smi312-negative processes (sh-p75: 37% ± 2% none versus 40% ± 4% single; Cre-GFP: 38% ± 4% none versus 42% ± 4% single) after 7 div. Figure 5D shows sequential images of a typical transfected progenitor cell with sh-p75 that divided into two newborn neurons (see also Movie S6). One of the newborn neurons grew processes of similar length after 7 div but did not initiate axonal growth, as determined by Smi312 staining in a postfixed preparation.

We reasoned that the partial axonal phenotype elicited in the experiments above (Figure 5B) might be caused by incomplete downregulation of $p75^{NTR}$ at a time critical for polarization. To tackle this issue, we established experimental paradigms in which $p75^{NTR}$ is knocked out in proliferating progenitors for the time necessary to reliably deplete the receptor before cells differentiate in polarized neurons. To obtain consistent $p75^{NTR}$ depletion in the nascent neurons, we maintained cells transfected with Cre-GFP in a proliferative state for 10 div before we induced differentiation by growth-factor withdrawal for additional 7 div (Figure 5C). Using this approach, Dcx-positive neurons lacking the axon drastically increased (56% ± 2% none versus 27% ± 2% single) in comparison to control (17% ± 6% none versus 64% ± 4% single), indicating that strong depletion of $p75^{NTR}$ during early polarization of newborn neurons results in important axonal phenotype.

$p75^{NTR}$ Is Required to Initiate Axons in Adult-Generated Neurons of the Hippocampus In Vivo

We next investigated whether $p75^{NTR}$ regulates axogenesis of newborn neurons in vivo. Neurons in the dentate gyrus of the adult hippocampus showed $p75^{NTR}$ expression at a very early stage of differentiation, suggesting that the receptor is specifically required at the time of polarity breaking. To visualize $p75^{NTR}$ expression in newborn neurons, we injected adult mice with a retroviral vector that only integrates into actively dividing precursor cells (Tashiro et al., 2006). This procedure labels newborn neurons by inducing reporter gene expression (i.e., retro-GFP) and allows establishment of approximate neuronal age (Figure S1A). Following in vivo neurogenesis, GFP-positive newborn neurons were analyzed at 3, 5, 7, 12, and 21 days postinjection (dpi). Immunostaining of $p75^{NTR}$ during early stages of newborn neuron differentiation revealed that $p75^{NTR}$ expression increased from 3 to 7 dpi and it was asymmetrically enriched at the membrane-initiation site of axon fibers and at proximal axon segments (Figure 6A). At 12–21 dpi, when axons reaching the inner margin of the CA3 area were clearly discernible (Figure S1A), total expression of $p75^{NTR}$ dropped and its asymmetrical distribution was lost (Figure 6A).

For in vivo manipulation of $p75^{NTR}$ expression, we first used lentiviral expression, which transduces neurons with a very high efficiency (van Hooijdonk et al., 2009). When delivered to the subgranular zone, this lentiviral system preferentially targets all progenitor cells and their neuronal progeny, but not mature granule neurons. Nevertheless, lentiviral vectors do not limit transduction to adult-generated neurons from birth (van Hooijdonk et al., 2009). Therefore, to specifically focus our analysis on newborn neurons prior to polarization, we coinjected mice with a lentivirus transducing scrambled shRNA or sh-p75 together with a retrovirus transducing an RFP reporter gene to allow birth-dating assessment. After 21 dpi, we found that the percentage of cells with radial morphology and discernible axons differed between control and sh-p75-expressing cells (Figure 6B). In particular, following lenti-sh-p75 injection, we observed an overall polarity phenotype characterized by an increased percentage of neurons lacking the axon (60% ± 10%) compared to control cells (8% ± 9%). Conversely, the number of neurons expressing a single axon decreased (27% ± 4%) in sh-p75-expressing cells versus controls (86% ± 10%). The number of cells displaying a horizontal shape did not significantly change (Figure 6B).

Next, we injected retro-GFP or retrovirus transducing Cre-recombinase (retro-Cre-GFP) into the dentate gyrus of $p75^{lox/lox}$ mice. We found that expression of $p75^{NTR}$, defined by $p75^{NTR}$/GFP colocalization, was similar in neurons transducing GFP and Cre-GFP at 3 dpi (Figure S1B), indicating that gene deletion does not affect the receptor expression levels at this early time point in vivo. At 7 dpi, while control neurons significantly increased $p75^{NTR}$ expression, Cre-neurons failed in upregulating $p75^{NTR}$ expression (Figure S1B). Next, we linked basal receptor expression with deficient axogenesis in single Cre neurons. When we examined hippocampal sections at 21 dpi (Figure 6B), the number of Cre neurons that displayed impaired polarization correlated with the number of neurons that originally expressed low $p75^{NTR}$ levels. Thus, newborn neurons likely require threshold levels of $p75^{NTR}$ at the critical time of polarity breaking (3–7 dpi) to promote axogenesis.

To obtain extensive $p75^{NTR}$ depletion in the nascent neurons, we induced *$p75^{NTR}$* gene deletion directly in progenitor cells of the adult dentate gyrus. To this end, homozygous $p75^{lox/lox}$ mice were crossed with a mouse line expressing the tamoxifen-inducible form of Cre (CreERT2) in the locus of the astrocyte-specific glutamate transporter (GLAST) (Mori et al., 2006). To visualize the recombined cells, we additionally crossed $p75^{lox/lox}$-Cre mice with transgenic mice expressing β-galactosidase (β-gal) reporters. Because *$p75^{NTR}$* gene deletion is permanent in progenitors upon tamoxifen induction and neurogenesis is a continuous process in the dentate gyrus, these mice allowed us to study newborn neurons generated from progenitor cells after assessment of $p75^{NTR}$ depletion. Mice were induced with tamoxifen for 5 days and injected with retro-GFP only 10 days

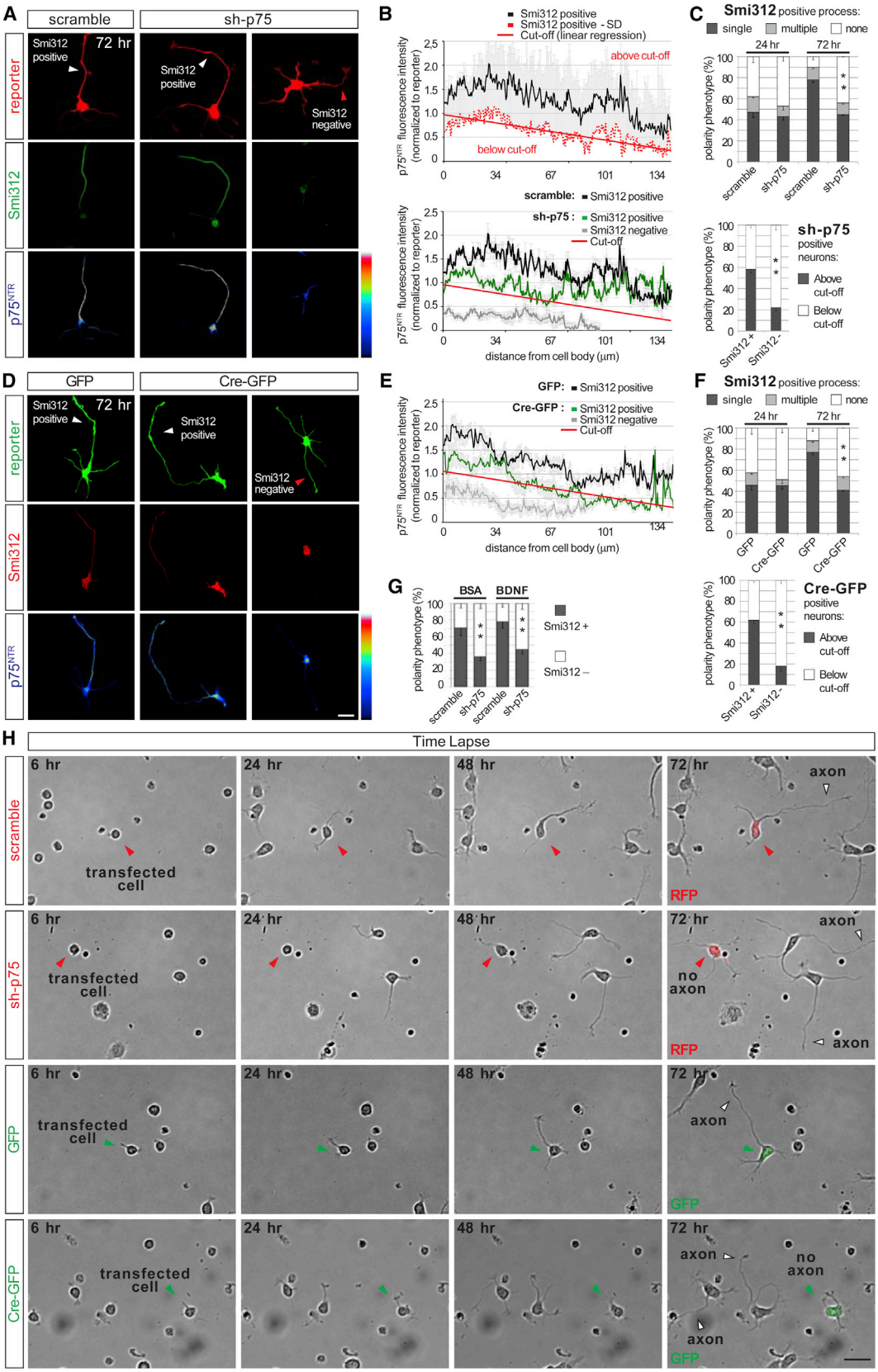

(legend on next page)

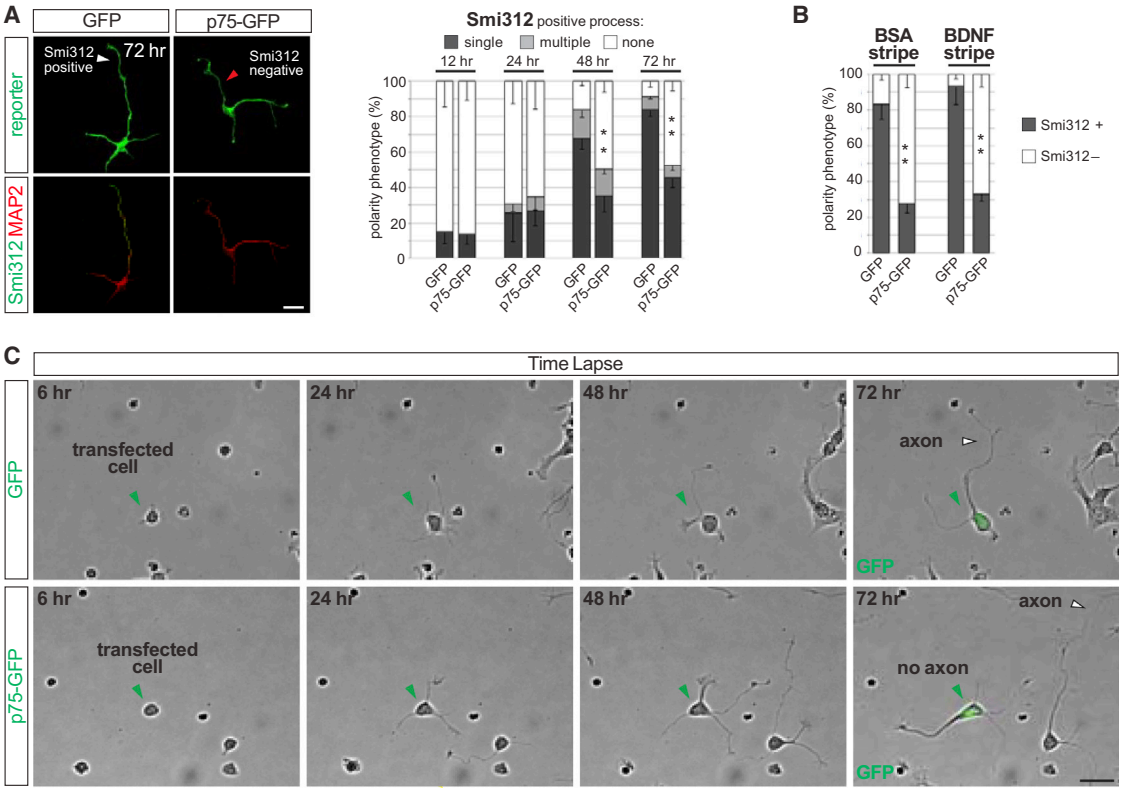

Figure 4. Ectopic p75^{NTR} Expression Affects Neuronal Polarization In Vitro

(A) Neurons transfected with either GFP or p75-GFP vectors stained for MAP2 or Smi312. Percentage of GFP or p75-GFP neurons expressing single, multiple, or no axons. Data depict average percentage (±SEM) from five different cultures (~50 cells each) for each time point (**$p < 0.01$).

(B) Neurons transfected with GFP or p75-GFP, cultured on BSA and BDNF stripes, and stained for Smi312 after 72 hr. Data depict average percentage (±SEM) from seven different cultures (~30 cells each) (**$p < 0.01$).

(C) Sequential images of neurons transfected with GFP or p75-GFP. Fluorescence signal confirmed reporter expression at the end of the recording. Scale bar represents 15 μm.

after tamoxifen induction (Figure 6C). This latency was sufficient to reduce residual p75^{NTR} protein following gene deletion by injection with tamoxifen (data not shown). Mice were then perfused at 21 dpi and GFP/β-gal-positive cells were quantified according to the presence of their axonal projections. In control mice, we found that neurons with a bipolar shape showed one axon (88% ± 2%) reaching the CA3 region. By contrast, Cre recombination in p75$^{lox/lox}$-Cre mice caused a striking decrease in the number of neurons forming an axon (26% ± 5%) with very little and thin axon fibers found in the CA3 region (Figure 6C). Conversely, the majority of recombined neurons (71% ± 4%) extended multiple small processes characterized by a large tip

Figure 3. Disruption of Polarized Localization of p75^{NTR} Affects Axonal Specification

(A) Neurons transfected with scrambled shRNA or sh-p75 vectors stained for Smi312 and p75^{NTR}. Scale bar represents 10 μm.

(B) Fluorescence cutoff level (linear regression) defined as mean p75^{NTR} intensity profile of scrambled shRNA cells normalized to that of RFP (reporter) and subtracted of SD. Lower graph shows p75^{NTR} intensity-profile averages of Smi312-positive (green) and Smi312-negative (gray) processes in sh-p75 cells. Profile of scramble shRNA cells and cutoff levels are also shown. Data depict average percentage (±SD) from seven different cultures (~40–50 cells each).

(C) Percentage of scrambled shRNA or sh-p75 neurons expressing single, multiple or no axons (upper histogram). Percentage of sh-p75 neurons expressing single axon (Smi312+) or lacking an axon (Smi312–) after 72 hr that show p75^{NTR} immunoreactivity above or below cutoff levels (lower histogram). Data depict average percentage (±SEM) from eight different cultures (~30–40 cells each) for each time point (**$p < 0.01$).

(D) Neurons from p75$^{lox/lox}$ mice transfected with GFP or Cre-GFP vectors and stained in (A).

(E) p75^{NTR} intensity-profile averages in GFP or Cre-GFP cells as depicted in (B). Data depict average percentage (±SD) from seven different cultures (~40–50 cells each).

(F) Polarity phenotype quantification in GFP or Cre-GFP neurons as depicted in (C). Data depict average percentage (±SEM) from five different cultures (~50 cells each) for each time point (**$p < 0.01$).

(G) Neurons transfected with scrambled shRNA or sh-p75 cultured on BSA and BDNF stripes and stained for Smi312 after 72 hr (**$p < 0.01$).

(H) Sequential images of neurons transfected with scrambled shRNA and sh-p75 or GFP and p75-GFP. Fluorescence signal confirmed reporter expression at the end of the recording. Scale bar represents 15 μm.

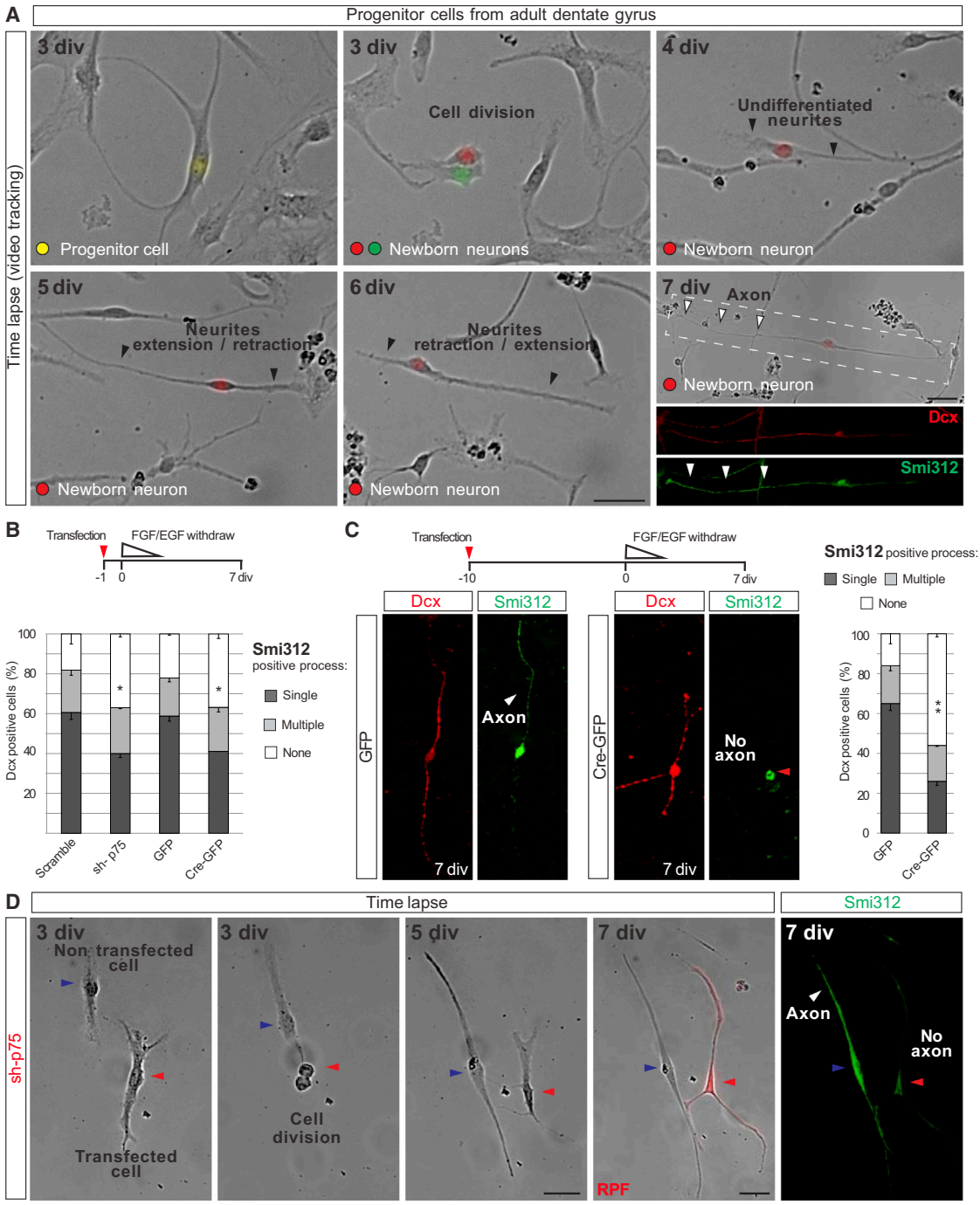

Figure 5. p75^{NTR} Specifies Axons in Newborn Neurons In Vitro

(A) Sequential images of a progenitor cell (yellow) that generated two immature neurons (red and green). Scale bar represents 20 μm.

(B) Schematic diagram illustrating the experimental protocol used to knockout/ knockdown p75^{NTR} in newborn neurons in vitro. Histogram shows the percentage of newborn neurons (Dcx positive), transfected with scrambled shRNA or sh-p75 and GFP or Cre-GFP constructs, showing single, multiple, or no Smi312-positive axons after 7 div (*$p < 0.05$). Data depict average percentage (±SEM) from four different cultures (~50 cells each).

(C) Newborn neurons transfected with GFP or Cre-GFP and stained for Dcx and Smi312 after 7 div. Differentiation was induced by FGF/EGF withdraw 10 div after transfection. Data depict average percentage (±SEM) from six different cultures (~50 cells each) (**$p < 0.01$).

(D) Sequential images showing a neuron transfected with sh-p75. The RFP signal is shown at the end of the recording. Scale bar represents 20 μm.

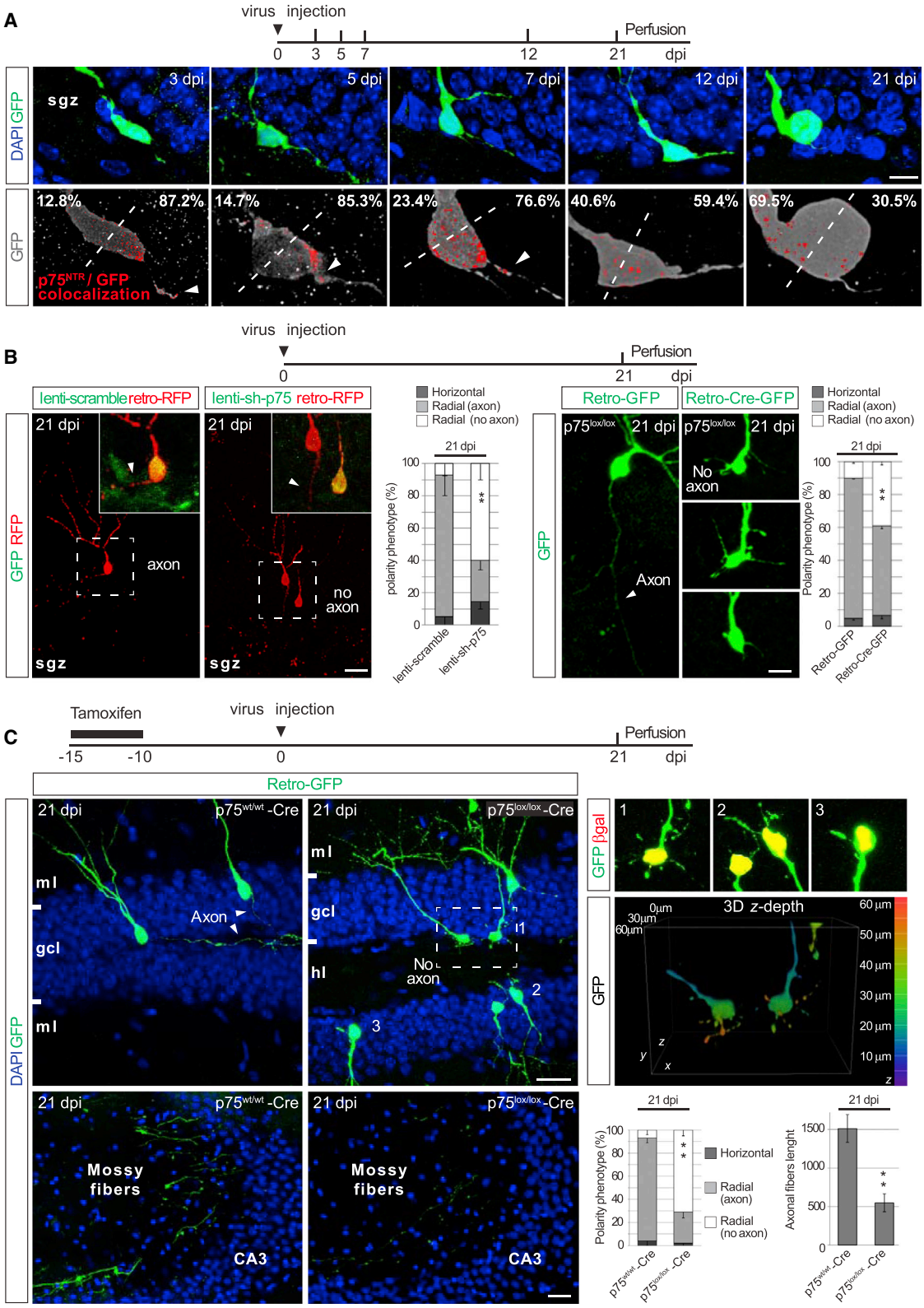

(legend on next page)

that ended at a short distance from the cell body, as revealed by three-dimensional reconstruction images (Figures 6C; see also Figures S1C and S1D). Thus, neurons in which $p75^{NTR}$ were efficiently downregulated at early stages showed bipolar shape and dendrite formation at 21 dpi, but they lacked one axon.

Finally, we overexpressed $p75^{NTR}$ in vivo by retroviral transduction of p75-GFP in newborn neurons and showed that axogenesis was impaired following adult neurogenesis (Figure S2A).

$p75^{NTR}$ Is Required for Neuronal Polarity in the Developing Neocortex In Vivo

We addressed the role of $p75^{NTR}$ during neuronal polarization in the developing brain in vivo. We utilized in utero electroporation (Saito and Nakatsuji, 2001) to interfere with endogenous $p75^{NTR}$ expression in ventricular precursor cells and their neuronal progeny. Constructs encoding either scrambled shRNA or sh-p75 were injected into the lateral ventricle of E17 rat embryos and electroporated into a subpopulation of layer II/III pyramidal-neuron progenitors (Figures 7A and 7B). To compare the number of cells electroporated in different animals, embryos were cotransfected with a separate vector expressing the reporter (GFP) only. In a second set of experiments, we also electroporated constructs encoding either GFP or Cre-GFP in $p75^{lox/lox}$ mice embryos at E15.5 (Figures 7D and 7E). Following electroporation, embryos were returned to the abdominal cavity of the dam and allowed to develop for an additional 5 (E21, rats) or 3 (E18.5, mice) days. Detailed analysis of embryonic brain slices revealed that control neurons (scrambled shRNA or GFP) progressively migrated through the intermediate zone (iz) to find their final location at the cortical plate (cp). At the upper iz and cp, neurons exhibited the typical bipolar morphology of migrating neurons (Kriegstein and Noctor, 2004), characterized by one short and thick neurite extending toward the cp (leading process, the future apical dendrite) and another thin and long neurite growing in the opposite direction (trailing process, the future axon). Compared to control neurons (6% ± 4% no axon, 86 ± 6 single axon, 8 ± 4 multiple axons; 18% ± 1% no axon, 80 ± 1 single axon, 2 ± 1 multiple axons), the number of sh-$p75^{NTR}$-transfected (32% ± 3% no axon, 61 ± 4 single axon, 7 ± 2 multiple axons) or Cre-GFP-transfected (34% ± 2% no axon, 64 ± 2 single axon, 2 ± 1 multiple axons) neurons exhibiting a single axon significantly decreased (Figures 7A and 7D).

At P7, pyramidal neurons derived from progenitors transfected with control constructs were mostly located at their final destination in layer II/III of the cp. Cortical-neuron axons were well developed, with radial orientation toward deep cortical layers (area 1, proximal fibers) (Figures 7C and 7F), and after reaching the white matter (area 2, ipsilateral fibers) the axons projected to the contralateral cortex (Figure 7C). In contrast to controls, neurons electroporated with sh-p75 or Cre-GFP showed a decrease in the number of axonal fibers at both locations (Figures 7C and 7F), as shown by the strong reduction in fluorescence labeling of proximal and ipsilateral axon fibers.

Electroporation of neuronal progenitors with p75-GFP resulted in similar defective axogenesis in the developing cortical network (Figures S2B–S2D).

DISCUSSION

Threshold Levels of $p75^{NTR}$ Are Required at the Time of Polarity Breaking to Orchestrate Axonal Specification

Our in vitro data indicate that threshold $p75^{NTR}$ expression correlates with the phenotype of sh-p75 and Cre-GFP neurons. Depending on the efficiency of shRNA or Cre recombination obtained in different experimental systems, we report high correlation between reduced $p75^{NTR}$ expression and the lack of axogenesis (Figures 3C and 3F). Given this correlation in vitro, we hypothesized that the incomplete axonal phenotype that we described in our in vivo studies may depend on the incomplete downregulation of $p75^{NTR}$ by sh-p75 (Figure 7A) or Cre-GFP (Figures 6B and 7D). In agreement with this hypothesis, we found an increasing number of cells with no axons by treatments that ensured increasingly stronger depletion of $p75^{NTR}$ (Figure 6C). That $p75^{NTR}$ levels are important for neurotrophin-mediated axonal polarization is also strengthened by the temporal and spatial expression patterns of the receptor in adult-born neurons in vivo. We observed that endogenous $p75^{NTR}$ showed localized expression at the pole of axon initiation 3, 5, and 7 days after neuronal birth, with expression decreasing after 12 days (Figure 6A). Strikingly, high $p75^{NTR}$ expression also correlated with its requirement for axonal specification. As demonstrated by $p75^{NTR}$ knockout experiments in $p75^{lox/lox}$ animals during adult neurogenesis, the time between 3 and 7 dpi was decisive in linking $p75^{NTR}$ expression and axogenesis in newly generated neurons. Hence, direct deletion of $p75^{NTR}$ in progenitor cells followed by long-lasting depletion (10 days) of the residual receptor resulted in strike reduction of axon fibers formation in their neuronal progeny after 21 dpi (Figure 6C). Such a dramatic effect

Figure 6. Knockout $p75^{NTR}$ Abolishes Axon Formation in Adult-Generated Neurons In Vivo

(A) Newborn neurons expressing GFP in adult mice injected with retro-GFP and perfused at 3, 5, 7, 12, and 21 dpi. $p75^{NTR}$/GFP fluorescence colocalization (red) is superimposed to that of GFP (gray). Arrowheads indicate $p75^{NTR}$/GFP colocalization in the proximal part of the axons. The percentage of colocalizing pixels is reported for each half of the cell bodies divided by the dashed line. Scale bar represents 10 μm.

(B) Newborn neurons double transduced with retro-RFP and lenti-scrambled shRNA or lenti-sh-p75. Insets (3× magnification) show single-transduced (red) and double-transduced (yellow) neurons. Scale bar represents 20 μm. The histogram shows the percentage of newborn neurons with single or no axon. Data depict average percentage (±SEM) from three different preparations (~20 cells each) (**$p < 0.01$). On the right are newborn neurons from $p75^{lox/lox}$ mice transduced with retro-GFP or retro-Cre-GFP. The histogram shows the percentage of newborn neurons with single or no axon. Data depict the average percentage (±SEM) from three different preparations (~80 cells each) (**$p < 0.01$). Scale bar represents 10 μm.

(C) Coronal section of the dentate gyrus from $p75^{wt/wt}$-Cre and $p75^{lox/lox}$-Cre mice 21 dpi. Lower panels show mossy fiber reaching the CA3 area in the same mice. Right panels show newborn neurons 1 to 3 from $p75^{lox/lox}$-Cre mice; GFP (green) and βgal (red) colocalization (yellow) is shown. A three-dimensional reconstruction of a representative area (dashed rectangle) shows neurons extending short processes that failed to exceed xyz axes (x = 85 mm, y = 70 mm, z = 60 mm). z depth is measured by pseudocolor scale. The histogram shows the percentage of newborn neurons with single or no axon. Terminal fibers reaching the CA3 region were also quantified. Data depict the average percentage (±SEM) from four different preparations (~80 cells each) (**$p < 0.01$). Scale bar represents 20 μm.

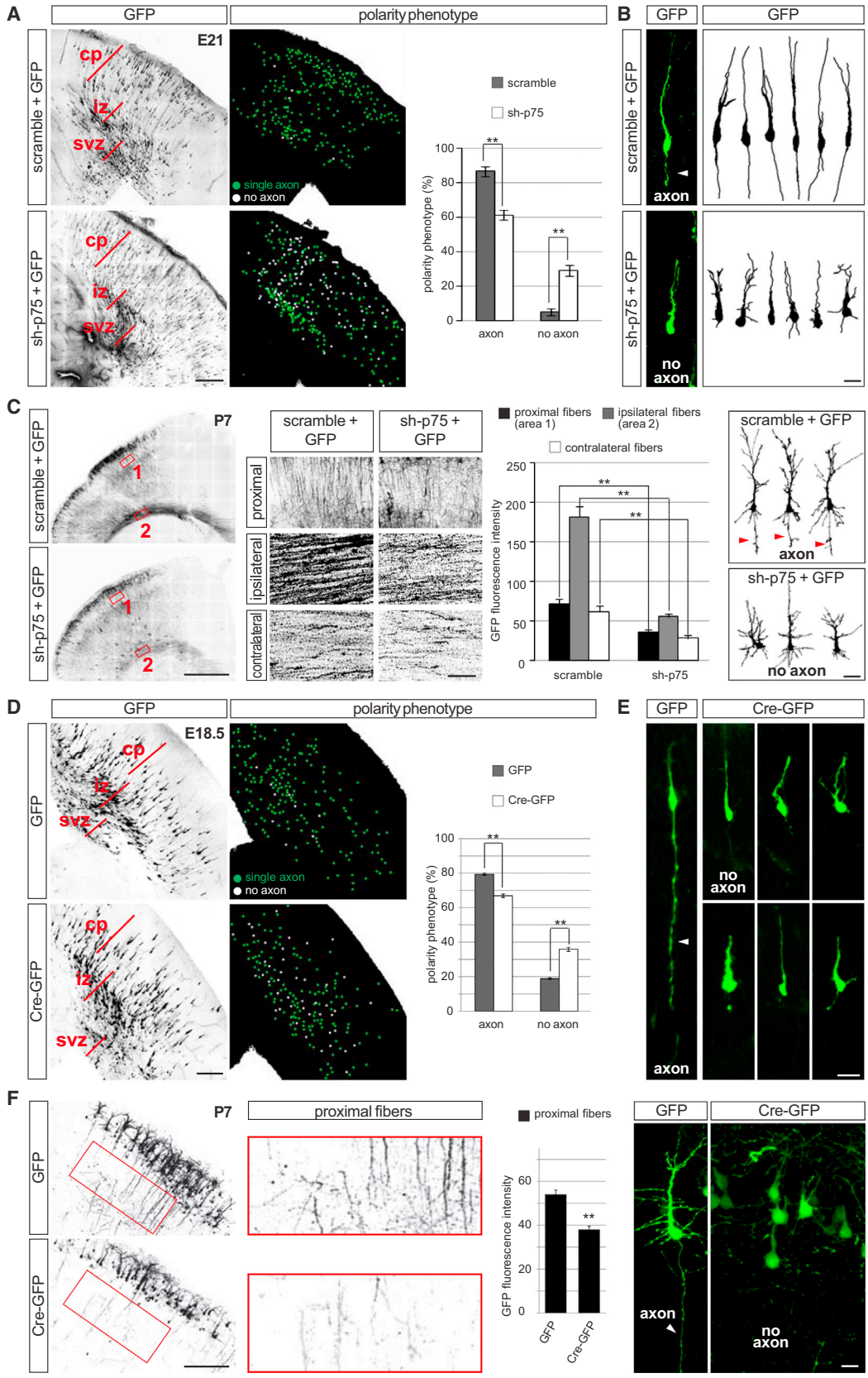

(legend on next page)

was not observed when depletion of $p75^{NTR}$ was incomplete at the time of polarity breaking, as observed by injecting retro-Cre-GFP in the dentate gyrus of $p75^{lox/lox}$ animals (Figure 6B). Likely, this also applies to ventricular precursor cells electroporated in utero with Cre-GFP constructs (Figures 7D and 7E).

Given the tight correlation between $p75^{NTR}$ expression level and axonal phenotype, it is intriguing that neurons in conventional knockout mice lacking $p75^{NTR}$ (p75 KO) do not exhibit an obvious defect in axon formation. Although direct assessment of axogenesis has never been investigated in p75 KO animals, we speculate that overriding polarizing signals could compensate for $p75^{NTR}$ deficiency throughout in vivo development. This was observed also for a number of other molecules regulating neuronal polarity in vivo (Reiner and Sapir, 2009; Cheng et al., 2011; Shelly et al., 2011). Indeed, acute downregulation of Dcx, MARK2, Sema3A, and Smurf1 proteins by in utero electroporation affects axonal specification, whereas mice deficient in these proteins present grossly normal neuronal polarization. Our experiments using conditional $p75^{lox/lox}$ mice, in which acute deletion of *p75*^{NTR} gene is cell specific and regulated in time, supported this hypothesis. Hence, our results reveal a significant phenotype: newborn neurons from $p75^{lox/lox}$ mice lack a single axon (Figures 6C and 7D). Moreover, these data are consistent with the polarity phenotype observed by knocking down $p75^{NTR}$ in vivo (Figures 6B and 7A). Polarity regulation by $p75^{NTR}$ is therefore conserved in all investigated experimental paradigms in vivo.

Positive-Feedback Modulation of $p75^{NTR}$ Expression Stabilizes Local Neurotrophin Signals for Axon Specification

How does $p75^{NTR}$ accumulate in just one neurite? $p75^{NTR}$ is involved in polarized vesicular transport in epithelial cells (Roux and Barker, 2002). In these polarized cells, vesicular sorting of $p75^{NTR}$ takes place at the *trans*-Golgi network, and the protein is constitutively delivered to the apical surface (Yeaman et al., 1997; Jareb and Banker, 1998). It was proposed that apical plasma membranes of epithelial cells correspond to the axon in a neuron. Although the analogy may be simplistic, one can speculate that vectorial/constitutive sorting of $p75^{NTR}$ may be followed by anterograde transport, which would account for axonal accumulation of the receptor. Therefore, the most conservative conclusion derived from our observations about $p75^{NTR}$ accumulation at the nascent axon is that the susceptibility of a neurite to be specified as an axon derives from vectorial $p75^{NTR}$ trafficking. However, our data provide an important molecular insight beyond $p75^{NTR}$ constitutive sorting: we found that local neurotrophins can orient the polarized distribution of $p75^{NTR}$. In stripe cultures, $p75^{NTR}$ preferentially accumulated in a single process following its contact with patterned neurotrophins (Figure 2C). The continuous $p75^{NTR}$ activation/accumulation loop represents a positive-feedback mechanism by which neurotrophins might orient $p75^{NTR}$ vesicular transport, ensuring that accumulation of the receptor remains confined to a single neurite (Figure 2D). Alternatively, neurotrophins could induce $p75^{NTR}$ accumulation at the nascent axon by in loco protein translation, as described for NGF-induced mPar3 synthesis during axonal elongation in dorsal root ganglia (Hengst et al., 2009).

Self-amplifying autocrine actions of BDNF have been initially discovered in the context of neuronal plasticity (Canossa et al., 1997, 2001; Krüttgen et al., 1998) and recently linked to axogenesis (Cheng and Poo, 2012). The continuous $p75^{NTR}$ activation/accumulation observed here together with the autocrine action of neurotrophins is in line with the idea that local positive-feedback loops generated by neurotrophins initiate a self-activation system that results in the morphological break of neuronal symmetry and consequent axonal specification (Arimura and Kaibuchi, 2007). Because the autocrine actions of BDNF are dependent on TrkB activation and recycling to the plasma membrane (Cheng et al., 2011; Cheng and Poo, 2012), it is possible that axonal specification elicited by neurotrophins requires also Trk receptors to ensure sufficient neurotrophin availability at the fated axon (Cheng and Poo, 2012). Nonetheless, in vivo experiments point to a minor role for Trk receptors in axon specification. Indeed, expression of a dominant-negative form of TrkB per se in newborn cortical neurons in vivo did not show an effect in neuronal morphological maturation, although a partial phenotype was found when TrkB dominant negative was transfected together with TrkC dominant negative (Nakamuta et al., 2011). Moreover, despite underdeveloped dendritic arborization, branching and spines formation, axogenesis, and the basic morphology of mossy fibers did not seem to be altered in TrkB-deficient newborn neurons (Bergami et al., 2008a). Figure S3 shows quantification analysis of axogenesis in TrkB-deficient newborn neurons in the dentate gyrus of the hippocampus in vivo. Thus, our in vitro and in vivo data suggest that $p75^{NTR}$ is

Figure 7. Knockout/Knockdown $p75^{NTR}$ Abolishes Axon Formation in Developing Cortical Neurons In Vivo

(A) Coronal section of the somatosensory cortex of E21 rat cortices transfected by in utero electroporation at E17 with GFP together with scrambled shRNA or sh-p75 vectors. cp, cortical plate; iz, intermediate zone; svz, subventricular zone. Scale bar represents 200 μm. The histogram shows the percentage of neurons showing a single axon or no axon. Data depict average percentage (±SEM) from 20 different embryos (**$p < 0.01$).

(B) Confocal images and 2D projection of typical cortical neurons from (A). Scale bar represents 10 μm.

(C) Coronal section of the somatosensory cortex of P7 rat cortices transfected as in (A). Scale bar represents 500 μm. High-magnification images of boxed region 1 (proximal fibers) and 2 (ipsilateral fibers) and contralateral fibers are shown. Scale bar represents 50 μm. The polarity phenotype is quantified as fluorescence intensity of axon fibers in boxed regions. Data depict average percentage (±SEM) from 20 different embryos. (**$p < 0.01$). At the far right are 2D projections of cortical neurons. Scale bar represents 10 μm.

(D) Coronal section of the somatosensory cortex of E18.5 mouse cortices transfected at E15.5 with GFP or Cre-GFP vectors. The histogram shows the percentage of neurons showing a single axon or no axon. Data depict average percentages (±SEM) from 30 different embryos (**$p < 0.01$).

(E) Confocal images of cortical neurons from (D). Scale bar represents 10 μm.

(F) Coronal section of the somatosensory cortex of P7 mouse cortices transfected as in (D). Scale bar represents 500 μm. High-magnification images of the boxed region show proximal fibers. The polarity phenotype is quantified as fluorescence intensity of axon fibers in boxed regions. Data depict average percentages (±SEM) from six different embryos. (**$p < 0.01$). At the far right are confocal images of cortical neurons. Scale bar represents 10 μm.

the primary receptor involved in neurotrophin-mediated axonal specification.

EXPERIMENTAL PROCEDURES

Cell Cultures

Dissociated hippocampal neurons were prepared from E17 mice as previously described (Santi et al., 2006). Neuronal precursor cultures were prepared from the dentate gyrus of adult mice (2 months old) and induced to differentiate as previously described (Babu et al., 2007). Cells were nucleofected using the Amaxa (Amaxa Bioscience) according to the manufacturer's instructions (see also Supplemental Experimental Procedures).

Substrate Micropatterning

Stripe-coated coverslips of fluorescently conjugated BSA (Invitrogen), BDNF, NGF, and NT-3 (Sigma) were prepared as previously described (Shelly et al., 2007) (see also Supplemental Experimental Procedures).

Fluorescent Microscopy and Immunocytochemistry/Histochemistry

Immunostaining of cultured hippocampal neurons, cultured neuronal progenitors, and brain slices were performed according to previously described standard procedures (Bergami et al., 2008b). Confocal imaging was performed using a laser-scanning motorized confocal system (Nikon A1) equipped with an Eclipse Ti-E inverted microscope and four laser lines (405, 488, 561, and 638 nm) (see also Supplemental Experimental Procedures).

Stereotaxic Surgery and In Utero Electroporation

Virus delivery into the dentate gyrus of adult mice was performed as previously described (Bergami et al., 2008a). Standard in utero electroporation was performed as previously described (dal Maschio et al., 2012) (see also Supplemental Experimental Procedures). All animals were used according to protocols by our institution licensing and the Italian Ministry of Health.

Time-Lapse Imaging

For live imaging, cell culture dishes were mounted on a dedicated stage incubator (OkoLab) and an Eclipse Ti-E inverted microscope (Nikon) equipped with a perfect focus system was used (see also Supplemental Experimental Procedures).

Statistical Analysis

Statistical analysis was carried out by using GraphPad Prism (GraphPad Software); Student's t test was used for assessing statistical significance. All data are reported as mean ± SEM. *$p < 0.05$; **$p < 0.01$.

SUPPLEMENTAL INFORMATION

Supplemental Information includes Supplemental Experimental Procedures, three figures, and six movies and can be found with this article online at http://dx.doi.org/10.1016/j.celrep.2014.02.039.

AUTHOR CONTRIBUTIONS

E.Z., M.B., and B.V. participated in the experimental design, performed most of the experiments, and discussed the results; G.B. performed the in utero experiments; B.A.P. provided $p75^{lox/lox}$ mice and discussed the results; S.S. performed the time-lapse experiments, prepared the figures, discussed the results, and provided financial support; L.C. supervised the in utero experiments, discussed the results, prepared the manuscript together with M.C., and provided financial support; and M.C. conceived and supervised the experiments, discussed results, prepared the manuscript and figures, and provided financial support.

ACKNOWLEDGMENTS

We thank Moses Chao and Louis F. Reichardt for providing blocking α-$p75^{NTR}$ antibody, Magdalena Götz for providing GlastCre::ERT2 mice, Rüdigher Kein for providing $TrkB^{lox/lox}$ mice, Fred Gage for providing CAG plasmids, Gerd Kempermann for providing neuronal precursor cells, Luca Berdondini for providing silicon wafer, and Giovanna Antonini for technical assistance. This work was supported by grants from the National Institutes of Health (R01 NS058510 to B.A.P.), Fondazione S. Paolo (to L.C.), Fondazione del Monte (to S.S.), MIUR, Progetto LIMONTE, and Fondazione S. Paolo (to M.C.).

Received: March 4, 2012
Revised: February 10, 2014
Accepted: February 20, 2014
Published: March 27, 2014

REFERENCES

Arimura, N., and Kaibuchi, K. (2007). Neuronal polarity: from extracellular signals to intracellular mechanisms. Nat. Rev. Neurosci. *8*, 194–205.

Babu, H., Cheung, G., Kettenmann, H., Palmer, T.D., and Kempermann, G. (2007). Enriched monolayer precursor cell cultures from micro-dissected adult mouse dentate gyrus yield functional granule cell-like neurons. PLoS ONE *2*, e388.

Barnes, A.P., Solecki, D., and Polleux, F. (2008). New insights into the molecular mechanisms specifying neuronal polarity in vivo. Curr. Opin. Neurobiol. *18*, 44–52.

Ben-Zvi, A., Ben-Gigi, L., Klein, H., and Behar, O. (2007). Modulation of semaphorin3A activity by p75 neurotrophin receptor influences peripheral axon patterning. J. Neurosci. *27*, 13000–13011.

Bergami, M., Rimondini, R., Santi, S., Blum, R., Götz, M., and Canossa, M. (2008a). Deletion of TrkB in adult progenitors alters newborn neuron integration into hippocampal circuits and increases anxiety-like behavior. Proc. Natl. Acad. Sci. USA *105*, 15570–15575.

Bergami, M., Santi, S., Formaggio, E., Cagnoli, C., Verderio, C., Blum, R., Berninger, B., Matteoli, M., and Canossa, M. (2008b). Uptake and recycling of pro-BDNF for transmitter-induced secretion by cortical astrocytes. J. Cell Biol. *183*, 213–221.

Bibel, M., and Barde, Y.A. (2000). Neurotrophins: key regulators of cell fate and cell shape in the vertebrate nervous system. Genes Dev. *14*, 2919–2937.

Bogenmann, E., Thomas, P.S., Li, Q., Kim, J., Yang, L.T., Pierchala, B., and Kaartinen, V. (2011). Generation of mice with a conditional allele for the p75(NTR) neurotrophin receptor gene. Genesis *49*, 862–869.

Cáceres, A., Ye, B., and Dotti, C.G. (2012). Neuronal polarity: demarcation, growth and commitment. Curr. Opin. Cell Biol. *24*, 547–553.

Canossa, M., Griesbeck, O., Berninger, B., Campana, G., Kolbeck, R., and Thoenen, H. (1997). Neurotrophin release by neurotrophins: implications for activity-dependent neuronal plasticity. Proc. Natl. Acad. Sci. USA *94*, 13279–13286.

Canossa, M., Gärtner, A., Campana, G., Inagaki, N., and Thoenen, H. (2001). Regulated secretion of neurotrophins by metabotropic glutamate group I (mGluRI) and Trk receptor activation is mediated via phospholipase C signalling pathways. EMBO J. *20*, 1640–1650.

Cheng, P.L., and Poo, M.M. (2012). Early events in axon/dendrite polarization. Annu. Rev. Neurosci. *35*, 181–201.

Cheng, P.L., Song, A.H., Wong, Y.H., Wang, S., Zhang, X., and Poo, M.M. (2011). Self-amplifying autocrine actions of BDNF in axon development. Proc. Natl. Acad. Sci. USA *108*, 18430–18435.

Craig, A.M., and Banker, G. (1994). Neuronal polarity. Annu. Rev. Neurosci. *17*, 267–310.

dal Maschio, M., Ghezzi, D., Bony, G., Alabastri, A., Deidda, G., Brondi, M., Sato, S.S., Zaccaria, R.P., Di Fabrizio, E., Ratto, G.M., and Cancedda, L. (2012). High-performance and site-directed in utero electroporation by a triple-electrode probe. Nat. Commun. *3*, 960.

Dechant, G., and Barde, Y.A. (2002). The neurotrophin receptor p75(NTR): novel functions and implications for diseases of the nervous system. Nat. Neurosci. *5*, 1131–1136.

Dotti, C.G., and Banker, G.A. (1987). Experimentally induced alteration in the polarity of developing neurons. Nature *330*, 254–256.

Dotti, C.G., and Banker, G. (1991). Intracellular organization of hippocampal neurons during the development of neuronal polarity. J. Cell Sci. Suppl. *15*, 75–84.

Gomis-Rüth, S., Wierenga, C.J., and Bradke, F. (2008). Plasticity of polarization: changing dendrites into axons in neurons integrated in neuronal circuits. Curr. Biol. *18*, 992–1000.

Goslin, K., and Banker, G. (1989). Experimental observations on the development of polarity by hippocampal neurons in culture. J. Cell Biol. *108*, 1507–1516.

Hengst, U., Deglincerti, A., Kim, H.J., Jeon, N.L., and Jaffrey, S.R. (2009). Axonal elongation triggered by stimulus-induced local translation of a polarity complex protein. Nat. Cell Biol. *11*, 1024–1030.

Huang, E.J., and Reichardt, L.F. (2001). Neurotrophins: roles in neuronal development and function. Annu. Rev. Neurosci. *24*, 677–736.

Huber, L.J., and Chao, M.V. (1995). Mesenchymal and neuronal cell expression of the p75 neurotrophin receptor gene occur by different mechanisms. Dev. Biol. *167*, 227–238.

Jareb, M., and Banker, G. (1998). The polarized sorting of membrane proteins expressed in cultured hippocampal neurons using viral vectors. Neuron *20*, 855–867.

Kaplan, D.R., and Miller, F.D. (2003). Axon growth inhibition: signals from the p75 neurotrophin receptor. Nat. Neurosci. *6*, 435–436.

Kriegstein, A.R., and Noctor, S.C. (2004). Patterns of neuronal migration in the embryonic cortex. Trends Neurosci. *27*, 392–399.

Krüttgen, A., Möller, J.C., Heymach, J.V., Jr., and Shooter, E.M. (1998). Neurotrophins induce release of neurotrophins by the regulated secretory pathway. Proc. Natl. Acad. Sci. USA *95*, 9614–9619.

Mi, S., Lee, X., Shao, Z., Thill, G., Ji, B., Relton, J., Levesque, M., Allaire, N., Perrin, S., Sands, B., et al. (2004). LINGO-1 is a component of the Nogo-66 receptor/p75 signaling complex. Nat. Neurosci. *7*, 221–228.

Mori, T., Tanaka, K., Buffo, A., Wurst, W., Kühn, R., and Götz, M. (2006). Inducible gene deletion in astroglia and radial glia—a valuable tool for functional and lineage analysis. Glia *54*, 21–34.

Nakamuta, S., Funahashi, Y., Namba, T., Arimura, N., Picciotto, M.R., Tokumitsu, H., Soderling, T.R., Sakakibara, A., Miyata, T., Kamiguchi, H., and Kaibuchi, K. (2011). Local application of neurotrophins specifies axons through inositol 1,4,5-trisphosphate, calcium, and Ca2+/calmodulin-dependent protein kinases. Sci. Signal. *4*, ra76.

Neukirchen, D., and Bradke, F. (2011). Neuronal polarization and the cytoskeleton. Semin. Cell Dev. Biol. *22*, 825–833.

Park, K.J., Grosso, C.A., Aubert, I., Kaplan, D.R., and Miller, F.D. (2010). p75NTR-dependent, myelin-mediated axonal degeneration regulates neural connectivity in the adult brain. Nat. Neurosci. *13*, 559–566.

Reiner, O., and Sapir, T. (2009). Polarity regulation in migrating neurons in the cortex. Mol. Neurobiol. *40*, 1–14.

Roux, P.P., and Barker, P.A. (2002). Neurotrophin signaling through the p75 neurotrophin receptor. Prog. Neurobiol. *67*, 203–233.

Saito, T., and Nakatsuji, N. (2001). Efficient gene transfer into the embryonic mouse brain using in vivo electroporation. Dev. Biol. *240*, 237–246.

Santi, S., Cappello, S., Riccio, M., Bergami, M., Aicardi, G., Schenk, U., Matteoli, M., and Canossa, M. (2006). Hippocampal neurons recycle BDNF for activity-dependent secretion and LTP maintenance. EMBO J. *25*, 4372–4380.

Schecterson, L.C., and Bothwell, M. (2008). An all-purpose tool for axon guidance. Sci. Signal. *1*, pe50.

Schecterson, L.C., and Bothwell, M. (2010). Neurotrophin receptors: old friends with new partners. Dev. Neurobiol. *70*, 332–338.

Shelly, M., Cancedda, L., Heilshorn, S., Sumbre, G., and Poo, M.M. (2007). LKB1/STRAD promotes axon initiation during neuronal polarization. Cell *129*, 565–577.

Shelly, M., Cancedda, L., Lim, B.K., Popescu, A.T., Cheng, P.L., Gao, H., and Poo, M.M. (2011). Semaphorin3A regulates neuronal polarization by suppressing axon formation and promoting dendrite growth. Neuron *71*, 433–446.

Singh, K.K., Park, K.J., Hong, E.J., Kramer, B.M., Greenberg, M.E., Kaplan, D.R., and Miller, F.D. (2008). Developmental axon pruning mediated by BDNF-p75NTR-dependent axon degeneration. Nat. Neurosci. *11*, 649–658.

Tahirovic, S., and Bradke, F. (2009). Neuronal polarity. Cold Spring Harb. Perspect. Biol. *1*, a001644.

Takahashi, D., Yu, W., Baas, P.W., Kawai-Hirai, R., and Hayashi, K. (2007). Rearrangement of microtubule polarity orientation during conversion of dendrites to axons in cultured pyramidal neurons. Cell Motil. Cytoskeleton *64*, 347–359.

Tashiro, A., Sandler, V.M., Toni, N., Zhao, C., and Gage, F.H. (2006). NMDA-receptor-mediated, cell-specific integration of new neurons in adult dentate gyrus. Nature *442*, 929–933.

Toriyama, M., Sakumura, Y., Shimada, T., Ishii, S., and Inagaki, N. (2010). A diffusion-based neurite length-sensing mechanism involved in neuronal symmetry breaking. Mol. Syst. Biol. *6*, 394.

van Hooijdonk, L.W.A., Ichwan, M., Dijkmans, T.F., Schouten, T.G., de Backer, M.W.A., Adan, R.A.H., Verbeek, F.J., Vreugdenhil, E., and Fitzsimons, C.P. (2009). Lentivirus-mediated transgene delivery to the hippocampus reveals sub-field specific differences in expression. BMC Neurosci. *10*, 2.

Walsh, G.S., Krol, K.M., Crutcher, K.A., and Kawaja, M.D. (1999). Enhanced neurotrophin-induced axon growth in myelinated portions of the CNS in mice lacking the p75 neurotrophin receptor. J. Neurosci. *19*, 4155–4168.

Wang, K.C., Kim, J.A., Sivasankaran, R., Segal, R., and He, Z. (2002). P75 interacts with the Nogo receptor as a co-receptor for Nogo, MAG and OMgp. Nature *420*, 74–78.

Weskamp, G., and Reichardt, L.F. (1991). Evidence that biological activity of NGF is mediated through a novel subclass of high affinity receptors. Neuron *6*, 649–663.

Wong, S.T., Henley, J.R., Kanning, K.C., Huang, K.H., Bothwell, M., and Poo, M.M. (2002). A p75(NTR) and Nogo receptor complex mediates repulsive signaling by myelin-associated glycoprotein. Nat. Neurosci. *5*, 1302–1308.

Wu, Q.F., Yang, L., Li, S., Wang, Q., Yuan, X.-B., Gao, X., Bao, L., and Zhang, X. (2012). Fibroblast growth factor 13 is a microtubule-stabilizing protein regulating neuronal polarization and migration. Cell *149*, 1549–1564.

Yamashita, T., and Tohyama, M. (2003). The p75 receptor acts as a displacement factor that releases Rho from Rho-GDI. Nat. Neurosci. *6*, 461–467.

Yeaman, C., Le Gall, A.H., Baldwin, A.N., Monlauzeur, L., Le Bivic, A., and Rodriguez-Boulan, E. (1997). The O-glycosylated stalk domain is required for apical sorting of neurotrophin receptors in polarized MDCK cells. J. Cell Biol. *139*, 929–940.